Thermal fluctuations of charge-density waves studied by NMR

J. Dolinšek and T. Apih
Jozef Stefan Institute, University of Ljubljana, Jamova 39, SLO-1000 Ljubljana Slovenia

K. Biljaković
Institute of Physics, Bijenička 46, P.O. Box 304, HR-10001 Zagreb, Croatia
(Received 19 February 1999)

Thermal fluctuations of a pinned incommensurate charge-density wave in zero external electric field were studied by NMR. Low-frequency random incoherent fluctuations of the amplitude and phase of the modulation wave affect the shape of the homogeneous decay of the transverse nuclear-spin magnetization. Phase fluctuations induce a characteristic exponential decay with the exponent proportional to the time variable as $t^{3/2}$ whereas the amplitude fluctuations result in a decay linear in t. The two types of fluctuations show very different temperature behavior. The phase fluctuations exhibit a weak T dependence and are present in the whole incommensurate phase, whereas the amplitude fluctuations are significant only in the close vicinity of the Peierls transition temperature, where they behave critically. The above effects are predicted on the basis of Landau theory using the assumption that the spectral density of phase fluctuations exhibits a central peak to account for the slow relaxational processes and memory effects in the presence of impurities. Theoretical predictions are compared to the ^{87}Rb NMR experiment in blue bronze $Rb_{0.3}MoO_3$, and a good agreement between the theory and experiment was found. The results show that the thermally induced phase fluctuations are slow and take place on a spatial scale of a small fraction of the charge-density-wave wavelength, thus on the subnanometric scale. [S0163-1829(99)13929-8]

I. INTRODUCTION

Fröhlich[1] predicted in the early 1950s that an incommensurate (INC) charge-density wave (CDW) could slide frictionless throughout the crystal lattice, representing a collective transport mechanism that could lead in perfect crystals to superconductivity. This situation was never encountered in real crystals where the impurities and commensurability potential of the underlying lattice pin the INC modulation wave and drastically restrict its translational degrees of freedom. A weak external dc electric field E of the order 10–100 mV/cm is, however, in many cases sufficient to depin the CDW and puts it into motion.[2] The resulting sliding modulation gives rise to a nonlinear electric conductivity[2,3] accompanied by a little understood coherent voltage noise in the I-V characteristics,[2–4] exhibiting well-defined Fourier components in the spectrum. The CDW sliding motion, under the electric field much larger than the threshold field E_T for depinning, was found to be coherent[2,5] with the phase coherence of the CDW extending to macroscopic distances. The drift velocity ν and the drift frequency ν_d of the coherently sliding CDW can be, to a good approximation, related by $\nu = \lambda \nu_d$, where λ is the CDW wavelength. At lower electric fields of the order $E \leqslant E_T$, the coherent motion transforms into a more stochastic one, accompanied by memory and hysteresis effects.[4] These effects are believed to result from the competing impurity pinning and electric-field depinning forces that frustrate the CDW and trap it into metastable states. It was argued that the pinning to impurities should result at $T=0$ in a spin-glass-like ordering[6] of the CDW, which breaks into domains that freeze with random phases relatively to each other.

The problem of CDW impurity pinning was studied by different models. In one approach, the electrically charged impurities are treated as static quenched,[7–9] located at random positions x_j and possessing a short-range Coulomb potential $V_0\delta(x-x_j)$ that interacts with (one-dimensional) charge density of the CDW condensate

$$\rho(x)=\overline{\rho}+\rho_0\cos[2k_Fx+\phi(x)]. \tag{1}$$

Here ρ_0 is the amplitude of the modulations wave and k_F the Fermi wave vector. The pinning energy at temperature $T=0$ in the absence of electric field was calculated to be[9,10]

$$\varepsilon_0=\{n_i\pi^2E_0(V_0\rho_0)^2m/m^*\}^{1/3}, \tag{2}$$

where n_i is the concentration of impurities, $E_0=\nu L^{-1}$ (L being a lattice constant), m is the free-electron mass and m^* the effective mass of the CDW condensate. A consequence of pinning is the vanishing of the nonlinear dc electrical conductivity[7,11] at $T=0$ and the introduction of a gap in the phason excitation spectrum.[12] An applied electric field below the threshold value effectively lowers the pinning energy and makes it vanish[11] at $E=E_T$. The electric-field depinning at $E\approx E_T$ can be regarded as a critical phenomenon.[13]

It has been argued that the assumption of mobile impurities[4] instead of static frozen might yield a better description of the pinned CDW. Here the mobile defects rearrange in a way to minimize their Coulomb interaction energy with the CDW by shifting in space for a small fraction of the CDW wavelength. Due to the CDW periodicity, the new arrangement of impurities also becomes periodic and forms the so-called defect density waves[14] (DDW). The description of the CDW motion in a periodic DDW potential, where the CDW moves in the presence of an electric field $E \leqslant E_T$ by

sudden phase slips[15] of 2π, seems to explain the anomalous motional narrowing of the NMR spectrum[16] in NbS_3. This narrowing occurred at an unexpectedly high CDW drift frequency ν_d of 15 MHz instead of expected 30 kHz, corresponding to the width of the static ^{93}Nb NMR spectrum.

The above impurity-pinning models were derived for zero temperature ($T=0$) and neglect thermal fluctuations of the CDW due to the coupling to the lattice heat bath. Most of the experiments on CDW sliding under the electric field can be, however, still well explained on the basis of these zero-temperature models, demonstrating that thermal fluctuations are relatively unimportant for the CDW dynamics in the presence of a strong or moderate electric field. On the other hand, thermal fluctuations should play an essential role in the CDW dynamics in the absence of the electric field. It is believed that they provide a mechanism for selecting between different metastable states, which is absent at zero temperature. At finite temperature thermal fluctuations will drive the system out of the metastable states towards an overall ground state. Thermal fluctuations also effectively lower the temperature-dependent pinning energy $\varepsilon(T)$ and can cause thermal depinning of the CDW in an analogous way to the electric-field depinning. It was predicted in a self-consistent harmonic phonon approximation[10] that there should exist a ''depinning'' temperature T_p above which the pinning energy vanishes [$\varepsilon(T_p)=0$] and the modulation wave slides free. Thermal fluctuations also provide a mechanism for a possible rearrangement of mobile impurities into a periodic defect density wave. Consequently, the nonlinear dc electrical conductivity of a pinned CDW that is zero at $T=0$, is restored at finite temperature due to the thermal depinning and appears as a thermally activated process.[11]

The electric-field depinning of the CDW is rather easy to observe experimentally. There the modulation wave propagates with a constant average drift velocity along a given direction and gives rise to nonlinear effects in bulk transport quantities like the ac electrical conductivity $\sigma(\omega)$. Thermal depinning, on the other hand, is much more difficult to observe. It gives rise to stochastic motion with no preferred direction, so that the average drift velocity is zero and the bulk transport properties are basically unaffected. In addition, local spectroscopic methods like NMR show[5] that in the absence of an external electric field, the pinning drastically restricts the CDW translational degrees of freedom. The CDW is observed static within the experimental precision in the whole temperature range below the Peierls transition. If thermally induced motion of the modulation wave exists, it is performed on a spatial scale of a small fraction of the CDW wavelength, thus in the subnanometric region. The depinning frequencies can also be very slow, as demonstrated by the appearance of a central peak in the excitation spectrum,[12] so that the depinning process can appear quasistatic on the observation time scales of most spectroscopic techniques. Such small-scale slow molecular motions are difficult to observe experimentally and that seems to be the reason why there is no direct observation of the CDW thermal fluctuations reported so far. In this paper we present–to the best of our knowledge–the first direct observation of the CDW thermal fluctuations in blue bronze $Rb_{0.3}MoO_3$ by NMR spectroscopy. Random stochastic fluctuations of the amplitude and phase of the INC modulation wave time modulate the sinusoidal electric-field gradient (EFG) tensor at the positions of ^{87}Rb nuclei and result in a homogeneous decay of the transverse nuclear-spin magnetization that is proportional to time as $t^{3/2}$. The decay power coefficient $\frac{3}{2}$ is characteristic for a stochastic motion in a sinusoidal EFG and can be accurately measured in a spin-echo-decay experiment.

II. SPECTRAL DENSITY OF FLUCTUATIONS

At nonzero temperature the incommensurate CDW undergoes random stochastic fluctuations in the amplitude and phase. We assume a plane-wave–type modulation and disregard the possible soliton effects. The static ($T=0$) modulation $\rho_0 \cos 2k_F x$ (neglecting the trivial constant phase shift) has to be replaced by a time-dependent expression

$$\rho(x)=\overline{\rho}+[\rho_0+\Delta\rho(x,t)]\cos[2k_F x+\Delta\phi(x,t)], \tag{3}$$

where $\Delta\rho(x,t)$ and $\Delta\phi(x,t)$ represent the amplitude and phase fluctuations that have zero time average. We assume that the fluctuations are small and linearize Eq. (3),

$$\rho(x,t)\approx\overline{\rho}+\rho_0\cos 2k_F x+\Delta\rho(x,t)\cos 2k_F x + \rho_0\Delta\phi(x,t)\sin 2k_F x. \tag{4}$$

In the above linearized expression the amplitude and phase fluctuations are decoupled and represent normal excitations (amplitudons and phasons) of the INC phase. The inclusion of higher-order terms, however, couples the two types of excitations.

In the following we shall be interested in the spectral densities of the Fourier components $\eta(\omega,q)$ ($\eta=\rho,\phi$) of the fluctuations, defined by

$$\Delta\eta(x,t)=\sum_{\omega,q}\eta(\omega,q)\exp\{i(qx+\omega t)\}, \tag{5}$$

where q is the wave vector of the fluctuations. The spectral densities $\langle|\eta(\omega,q)|^2\rangle$ (the brackets $\langle\ \rangle$ designating a thermodynamic ensemble average) were computed within the Landau theory for an INC structure characterized by a two-component order parameter $Q=\rho\exp(i\phi)$. For an underdamped mode, damped with a constant factor γ [defined through the dissipation function $R=(\gamma/2)(\partial Q/\partial t)(\partial Q^*/\partial t)$] and possessing an effective mass μ [defined via the kinetic energy $K=(\mu/2)(\partial Q/\partial t)(\partial Q^*/\partial t)$] one obtains[17]

$$\langle|\rho(q,\omega)|^2\rangle=\frac{\Gamma k_B T}{\pi V\mu[(\omega^2-\Delta_A^2-\kappa q^2)^2+\Gamma^2\omega^2]}, \tag{6a}$$

$$\langle|\phi(q,\omega)|^2\rangle=\frac{\Gamma k_B T}{\pi V\rho_0^2\mu[(\omega^2-\kappa q^2)^2+\Gamma^2\omega^2]}. \tag{6b}$$

Here $\Gamma=\gamma/\mu$, V is the crystal volume, and Δ_A and κ are defined via the long-wavelength amplitudon and phason-dispersion relations

$$\omega_A^2(q)=\Delta_A^2+\kappa q^2, \tag{7a}$$

$$\omega_\phi^2(q)=\kappa q^2. \tag{7b}$$

The term $\Delta_A\propto(T_I-T)^{1/2}$ represents an intrinsic gap in the amplitudon spectrum whereas the phason branch [Eq. (7b)] is considered to be gapless. It is well known that a gapless phason can exist only in an ideal, defect-free INC structure, whereas in real systems impurities and commensurability effects introduce a finite gap in the phason branch. In our model we shall, however, keep using the gapless phason-dispersion relation due to the fact that a pronounced central peak was observed in many real CDW systems,[12] that should not exist in the presence of a gap. It is, however, straightforward to include the phason gap Δ_ϕ in Eq. (6b) by making a substitution $\kappa q^2\rightarrow\Delta_\phi^2+\kappa q^2$. Here we also mention that one can obtain the spectral densities for an overdamped mode by limiting the kinetic coefficient $\mu\rightarrow 0$ in Eqs. (6a) and (6b).

The NMR line shape will be affected by the low-frequency part of the spectral densities. If we exclude a narrow temperature region near the phase-transition point, all the quantities in the square bracket of Eq. (6a) can be neglected with respect to Δ_A (which is of the order of hard phonon frequencies), so that the amplitudon spectral density can be approximated by a white noise[18]

$$\langle|\rho(q=0,\omega=0)|^2\rangle=\frac{\Gamma k_BT}{\pi V\mu\Delta_A^4} \tag{8}$$

that is q and ω independent.

The phason fluctuations are, on the other hand, of relaxational character, i.e., the phason mode is overdamped.[17] In the most interesting region (small ω) Eq. (6b) yields[19]

$$\rho_0^2\langle|\phi(q,\omega)|^2\rangle=\frac{\Gamma k_BT}{\pi V\mu[\kappa^2q^4+\Gamma^2\omega^2]}, \tag{9}$$

describing a central peak with the half width at half height $\Delta\omega_{1/2}=\kappa q^2/\Gamma$. Like in the case of diffusive-type fluctuations, this width is proportional to q^2. Here it should be stressed that the phason spectral density of Eq. (9) is essentially independent of the effective mass μ. This can be easily verified by recalling that $\Gamma=\gamma/\mu$ and $\kappa=D/\mu$, where D is the coefficient of the invariant $|\partial Q/\partial x|^2$ (the elastic term) in the Landau thermodynamic potential.[17]

III. THE ADIABATIC NMR LINE SHAPE

The NMR resonance frequency $\Omega(x,t)$ of a quadrupolar nucleus at a site x in a sinusoidal EFG is related to the order parameter of the INC modulation $\rho(x,t)$ at that site.[20] In the simplest case this relation is linear,

$$\Omega(x,t)=\Omega_0+a\rho(x,t), \tag{10}$$

and $\rho(x,t)$ is given by Eq. (4). Random incoherent fluctuations of the CDW amplitude and phase will produce random fluctuations of the resonance frequency. Due to the incoherent nature of the fluctuations, the corresponding frequency changes are also stochastic and cannot be refocused in a spin-echo experiment. These fluctuations determine the homogeneous (adiabatic) shape of the NMR spectrum.

Following Abragam,[21] the free-induction decay $G(t)$ of the transverse nuclear-spin magnetization is obtained as

$$G(t)=\exp\{-i\Omega_0t\}\left\langle\left\langle\exp\left\{-i\int_0^t[\Omega(x,t')-\Omega_0]dt'\right\}\right\rangle\right\rangle_x. \tag{11}$$

The inner brackets of the symbol $\langle\langle\ \ \rangle\rangle_x$ represent a thermodynamic ensemble average, whereas the outer brackets $\langle\ \ \rangle_x$ represent the average over the static inhomogeneous distribution of resonance frequencies. For the case of the frequency-space relation given by Eq. (10), one gets[20] using $X=\cos 2k_Fx$,

$$\langle\ \ \rangle_x\Rightarrow\int_{-1}^{1}\frac{dX}{\sqrt{(1-X^2)}}. \tag{12}$$

The NMR spectrum $I(\omega)$ is obtained by taking a Fourier transform of $G(t)$,

$$I(\omega)=\int_0^\infty G(t)\exp\{i\omega t\}dt. \tag{13}$$

Inserting Eqs. (10) and (4) into Eq. (11) we get

$$G(t)=\exp\{-i\Omega_0t\}\langle\langle G_1(t)G_2(t)\rangle\rangle_x, \tag{14}$$

where

$$G_1(t)=\exp\{-ia\rho_0t\cos 2k_Fx\} \tag{15a}$$

and

$$G_2(t)=\exp\left\{-ia\int_0^t[\Delta\rho(x,t')\cos 2k_Fx+\rho_0\Delta\phi(x,t')\sin 2k_Fx]dt'\right\}. \tag{15b}$$

The term $G_1(t)$ represents the inhomogeneous free-induction decay and its Fourier transform determines the static inhomogeneous NMR line shape

$$I_{\mathrm{INH}}(\omega)=\frac{1}{\sqrt{1-[(\omega-\Omega_0)/\Omega_1]^2}}, \tag{16}$$

where $\Omega_1=a\rho_0\propto\sqrt{T_I-T}$. The spectrum exhibits a typical shape with two edge singularities at $\Omega_0\pm\Omega_1$ that are separated by $2\Omega_1$.

The term $G_2(t)$ represents the homogeneous decay and includes the effects of thermal fluctuations. We perform first the ensemble average by taking the order-parameter fluctuations to be stationary and Gaussian and use the relation[21]

$$\left\langle\exp\left\{-i\int_0^t\omega(t')dt'\right\}\right\rangle=\exp\left\{\left\langle-\frac{1}{2}\left[\int_0^t\omega(t')dt'\right]^2\right\rangle\right\}. \tag{17}$$

We get

$$\langle G_2(t)\rangle = \exp\left\{ -a^2\left[\sum_{\omega,q} \langle|\rho(\omega,q)|^2\rangle \frac{1-\cos\omega t}{\omega^2}\cos^2 2k_F x + \rho_0^2 \sum_{\omega,q} \langle|\phi(\omega,q)|^2\rangle \frac{1-\cos\omega t}{\omega^2}\sin^2 2k_F x\right]\right\}. \tag{18}$$

Here we took into account that phasons and amplitudons are normal excitations of the INC phase so that the cross terms of the type $\langle\rho\phi\rangle$ vanish. We perform next the summation over q by replacing the summation by an integration over half of the Brillouin zone between 0 and k_D,

$$\sum_q \rightarrow \frac{1}{2}\frac{V}{2\pi^2}\int_0^{k_D} q^2 dq, \tag{19}$$

where k_D is the Debye wave vector. We define

$$\langle|\eta(\omega)|^2\rangle = \frac{V}{4\pi^2}\int_0^{k_D}\langle|\eta(\omega,q)|^2\rangle q^2 dq, \quad \eta=\rho,\phi \tag{20}$$

and perform the integration using Eqs. (8) and (9). This yields for the amplitude fluctuations

$$\langle|\rho(\omega)|^2\rangle = \frac{\Gamma k_B T k_D^3}{12\pi^3\mu\Delta_A^4}, \tag{21}$$

whereas for the phase fluctuations we get an expression

$$\rho_0^2\langle|\phi(\omega)|^2\rangle = \frac{\Gamma k_B T}{4\pi^3\mu\kappa^2}\int_0^{k_D}\frac{q^2 dq}{(\Gamma\omega/\kappa)^2+q^4}. \tag{22}$$

The function under the integral sign in Eq. (22) is dropping off rapidly for large q, so that the upper limit of integration can be extended to infinity. Using the equality

$$\int_0^\infty \frac{x^2}{1+x^4}dx = \frac{\pi}{2\sqrt{2}}$$

we get

$$\rho_0^2\langle|\phi(\omega)|^2\rangle = \frac{k_B T\sqrt{\Gamma}}{8\sqrt{2}\pi^2\mu\kappa^{3/2}\sqrt{\omega}}. \tag{23}$$

After integrating over q we still have to perform the summation over ω. This yields the homogeneous free-induction decay of the form

$$\langle G_2(t)\rangle = \exp\{-(\lambda_A t)\cos^2 2k_F x - (\lambda_\phi t)^{3/2}\sin^2 2k_F x\}. \tag{24}$$

The amplitudon damping coefficient λ_A is easily obtained by using

$$\int_0^\infty \frac{1-\cos\omega t}{\omega^2}d\omega = \frac{\pi}{2}t,$$

whence we get

$$\lambda_A = \frac{a^2\Gamma k_B T k_D^3}{24\pi^2\mu\Delta_A^4} \propto \frac{T}{(T_I - T)^2}. \tag{25}$$

In the calculation of the phason damping constant λ_ϕ one encounters an integral of the form

$$\int_0^\infty \frac{1-\cos\omega t}{\omega^{5/2}}d\omega = \lim_{\delta\rightarrow 0}\frac{2}{3\delta^{3/2}} + t^{3/2}\frac{4}{3}\sqrt{\pi/2}, \tag{26}$$

where the first term on the right-hand side diverges, but does not depend on the time variable. This divergence is a consequence of the diverging phason spectral density [Eq. (23)] at $\omega\rightarrow 0$. We can keep this term finite by integrating from a small nonzero lower limit δ (thus leaving out the $\omega=0$ singularity) and find the damping constant λ_ϕ of the time-dependent phason-induced decay as

$$\lambda_\phi = \left(\frac{a^2 k_B T\sqrt{\Gamma}}{12\pi^{3/2}\mu\kappa^{3/2}}\right)^{2/3} \propto T^{2/3}. \tag{27}$$

Comparing the temperature dependencies of λ_A and λ_ϕ, we observe that the amplitude fluctuations are significant only in the close vicinity of the phase-transition temperature T_I, where they show critical behavior. The phase fluctuations are, on the other hand, relatively weakly temperature dependent and are present in the whole INC phase, thus also far away from T_I. These features reflect the fact that the spectral density of the amplitudon fluctuations contains low frequencies only in the close vicinity of T_I, where the amplitudon gap Δ_A comes close to zero, whereas the phason-induced central peak is present in the whole INC phase, showing only a weak T dependence.

Equation (24) shows that the amplitude and phase fluctuations result in different exponential decays of the transverse nuclear-spin magnetization. The amplitudon-induced decay is linear in the time t, whereas the phason-induced decay is proportional to $t^{3/2}$. $\langle G_2(t)\rangle$ can be measured directly as a decay curve of the transverse magnetization in a two-pulse spin-echo experiment. Since $\langle G_2(t)\rangle$ depends on the space coordinate x and thus via Eqs. (10) and (16) varies with frequency over the inhomogeneous NMR spectrum, one has to determine the spin-echo decay curves in a frequency-selective way at different points on the Fourier-transformed spectrum. The spectral edge singularities occur at the condition $2k_F x = n\pi$, so that $\cos 2k_F x = \pm 1$ and $\sin 2k_F x = 0$, and the spin-echo decay on the singularities is amplitudon induced. The middle of the inhomogeneous spectrum corresponds to the condition $2k_F x = (2n+1)\pi/2$ so that $\cos 2k_F x = 0$ and $\sin 2k_F x = \pm 1$, and the decay in the center is determined by the phase fluctuations. Since the importance of the amplitude fluctuations vanishes rapidly on going away from T_I, the spectrum is expected to show only the $t^{3/2}$ phason-induced damped at temperatures that are not very close to the transition point.

IV. RESULTS AND DISCUSSION

Thermal fluctuations of the CDW were studied in blue bronze $Rb_{0.3}MoO_3$ by ^{87}Rb NMR. Blue bronze undergoes a Peierls metal-to-semiconductor transition to an INC CDW state at $T_I = 182$ K. A monocrystal sample was placed in the

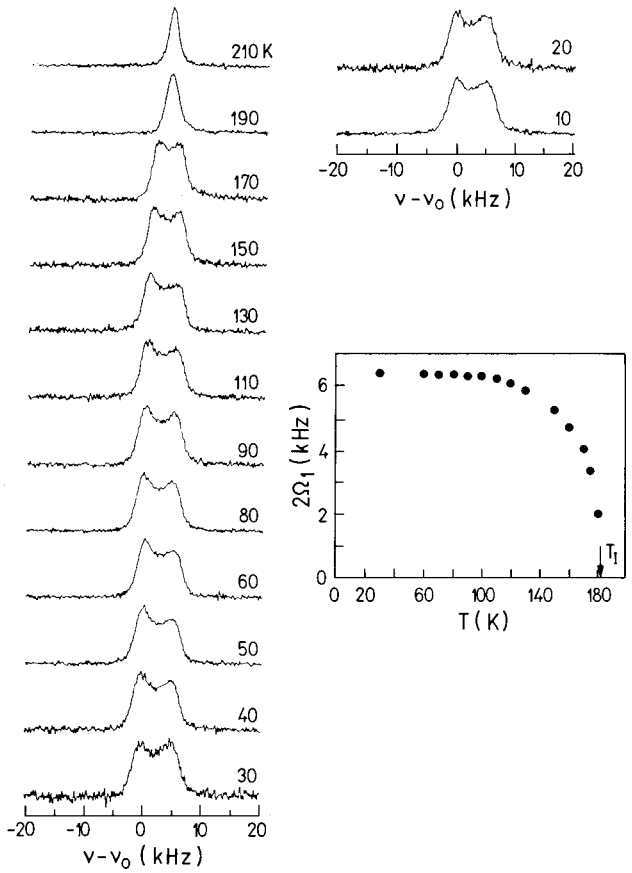

FIG. 1. Temperature dependence of the ^{87}Rb central transition NMR spectra (site two) of a $Rb_{0.3}MoO_3$ monocrystal, $\nu_0(^{87}\mathrm{Rb}) = 88.34$ MHz. The inset shows the temperature dependence of the splitting of the edge singularities.

magnetic field with the *b* axis (along which the CDW propagates) perpendicular to the field. The crystal was then rotated around *b* to a position where the resonance frequency depends linearly on the order parameter, so that the static inhomogeneous line shape can be described by Eq. (16). The ^{87}Rb central transition spectra (Rb site two)[5] are displayed in Fig. 1 as a function of temperature between 210 and 10 K. The inset shows the temperature dependence of the splitting $2\Omega_1$ of the edge singularities, which becomes nonzero at 182 K. The line shape is typical for the presence of a static INC modulation wave and shows an inhomogeneous broadening. The degree of this broadening was determined in a two-dimensional (2D) NMR experiment for the separation of inhomogeneous and homogeneous line shapes.[22] In this experiment the inhomogeneous and homogeneous lines appear separated in two orthogonal frequency domains of the 2D spectrum $I(\nu_1, \nu_2)$. The 2D experiment was performed at $T = 80$ K (Fig. 2). The ratio of the full widths at half height of the inhomogeneous (ν_2 domain) and homogeneous (ν_1 domain) spectra was found to be $\Delta\nu_{\mathrm{INH}}/\Delta\nu_{\mathrm{HOM}} = 122$, demonstrating that the spectrum is strongly inhomogeneously broadened. The observed static line shape already enables one to estimate the spatial scale on which the thermal fluctuations of the CDW—if present—are performed. The frequency splitting of the edge singularities corresponds via the frequency-space relation of Eq. (10) to half-wave length of the CDW in real space. In blue bronze the $\lambda/2 = \pi/2k_F$ wavelength at 80 K amounts to[23] about 0.5 nm. The CDW fluctuations on the spatial scale of the order of $\lambda/2$ with frequencies larger than the inhomogeneous spectrum width of 12 kHz would produce motional narrowing of the spectrum, and the typical double-horned static shape would be destroyed. The fact that the measured shape of the ^{87}Rb spectrum closely resembles the static line shape demonstrates that thermal fluctuations take place only on a scale of a small fraction of the CDW wavelength, that is on the subnanometric scale.

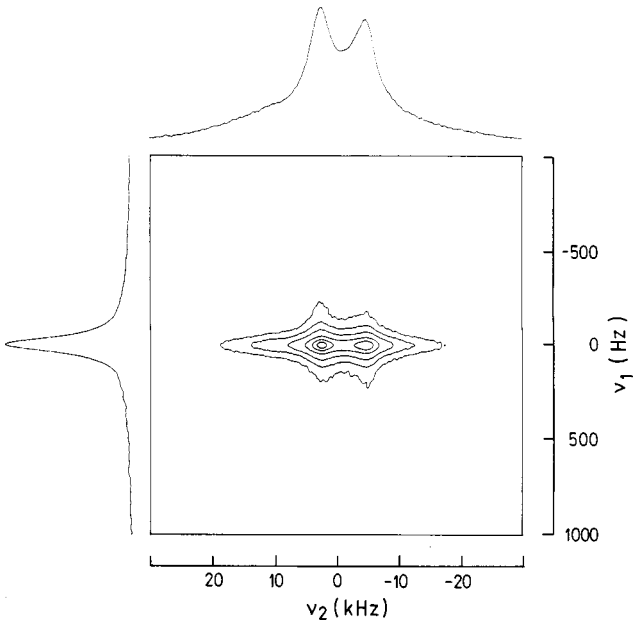

FIG. 2. ^{87}Rb 2D NMR spectrum of blue bronze at $T = 80$ K, showing separated inhomogeneous (ν_2) and homogeneous (ν_1) line shapes, $\nu_0(^{87}\mathrm{Rb}) = 88.34$ MHz.

The presence of slow dynamic processes in the INC phase of $Rb_{0.3}MoO_3$ was observed also in the temperature dependence of the ^{87}Rb NMR spin-lattice relaxation time T_1 (Fig. 3). It was predicted[20] that the phason fluctuations provide a very efficient spin-lattice relaxation mechanism in the INC phase, resulting in a very short and *T*-independent value of T_1 throughout the whole INC phase. Such a behavior is in-

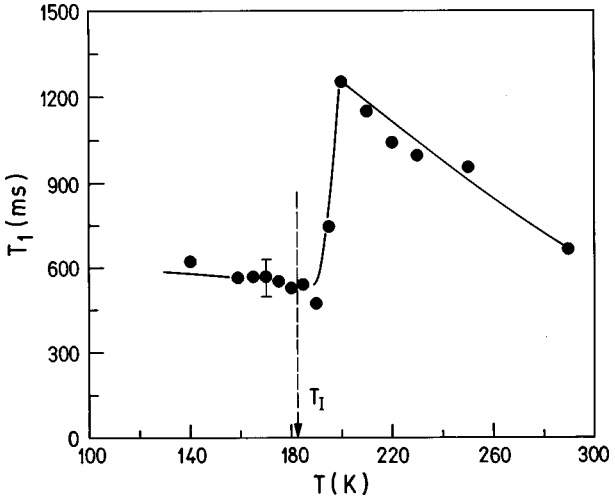

FIG. 3. Temperature dependence of the ^{87}Rb spin-lattice relaxation time T_1 in blue bronze. Solid line is a guide for the eye.

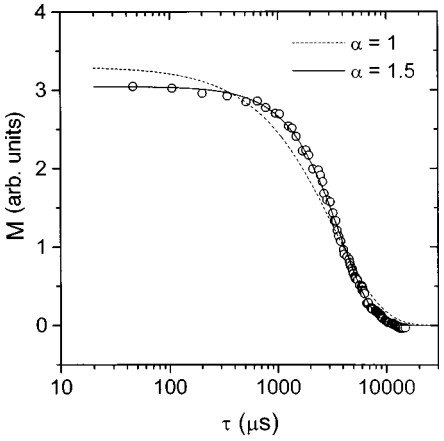

FIG. 4. A ^{87}Rb spin-echo decay curve at $T=110$ K in blue bronze. The solid line represents the fit with Eq. (28), yielding the decay exponent $\alpha=1.5$. A fit of the form $M(t)\propto\exp\{-\lambda t\}$ (dashed line), corresponding to the $\alpha=1$ case, is shown for comparison.

deed observed in Fig. 3. It is interesting that T_1 becomes short already more than 10 K above the actual transition temperature, demonstrating the existence of slow pretransitional dynamics. Similar effect was observed in blue bronze also in a neutron-scattering experiment,[12] where this slow pretransitional dynamic was attributed to the critical growth of the central peak and anomalous mode softening.

A conclusive evidence for the presence of thermal fluctuations was obtained from the measured spin-echo decay curves in a two-pulse Hahn echo experiment that yields the homogeneous free-induction decay function $\langle G_2(t)\rangle$. The time delay between pulses was varied over three orders of magnitude from 40 μsec up to several ten msec. The decay curves were determined in a frequency-selective manner from the spectra. A typical decay curve at $T=110$ K, obtained from the intensity in the middle of the spectrum, is displayed in Fig. 4. Experimental points were fitted with the ansatz

$$M(t)=M_0\exp\{-(\lambda_\phi t)^\alpha\}, \tag{28}$$

where the power coefficient α was treated as a fit parameter. The fit (solid line in Fig. 4) reproduces well the experimental data yielding the value $\alpha=1.48\pm0.05$ that is in perfect agreement with the theoretical value $\frac{3}{2}$, predicted for the mechanism of thermal phase fluctuations. A monoexponential fit ($\alpha=1$), which cannot reproduce the experimental points, is shown for comparison. The large difference between the $\alpha=1$ and $\frac{3}{2}$ curves demonstrates the high precision to which the exponent α can be determined. The temperature dependence of α is shown in Fig. 5(a). In the temperature range between 175 and 150 K, α amounts to about 1.65 that is slightly above the theoretical value 1.5, whereas below 150 K the average α value becomes almost perfectly 1.5. The temperature dependence of the damping coefficient λ_ϕ is displayed in Fig. 5(b). According to Eq. (27), λ_ϕ should depend on temperature as $T^{2/3}$. The best fit [solid line in Fig. 5(b)] was made with the ansatz $\lambda_\phi=A+BT^{2/3}$ that includes, in addition to the phason term, a temperature-independent contribution. The inclusion of the T-independent contribution is reasonable, as it implies that the homogeneous line at $T=0$ does not become infinitely sharp after vanishing of the

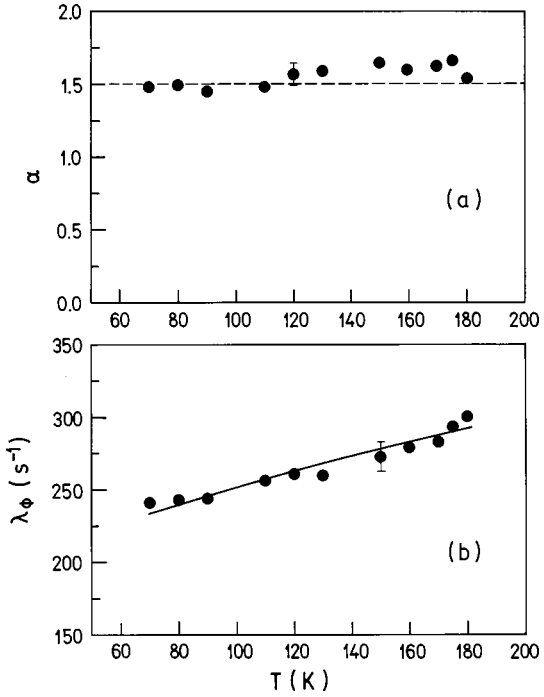

FIG. 5. (a) Temperature dependence of the decay exponent α. The theoretical value $\alpha=\frac{3}{2}$, characteristic for the mechanism of thermal phase fluctuations, is shown as a dashed line. (b) Temperature dependence of the damping constant λ_ϕ. Solid line is the fit with the Eq. (27) plus a T-independent term.

$BT^{2/3}$ term. The fit yielded the values $B=(a^2k_B\sqrt{\Gamma}/12\pi^{3/2}\mu\kappa^{3/2})^{2/3}=4.0\ \mathrm{s^{-1}K^{-2/3}}$ and $A=166.7\ \mathrm{s^{-1}}$. These values show that at, e.g., $T=150$ K the phase fluctuations-induced broadening contributes 40% to the total width of the homogeneous spectrum. In order to check for the frequency dependence of the parameters α and λ_ϕ, the analysis was made also on other parts of the inhomogeneous spectrum, but no significant variation over the spectrum was found. The T dependence of α also shows that the thermal phase fluctuations provide the dominant damping mechanism in the whole investigated temperature range, whereas the amplitude fluctuations were not detected. Such behavior is consistent with the prediction of the Eq. (25) and demonstrates that the amplitude-induced damping might be significant only in the close vicinity of T_I.

The above results demonstrate that the thermal phase fluctuations of the CDW in $Rb_{0.3}MoO_3$ exist in the whole measured temperature range ($\Delta T\approx110$ K) of the INC phase in contrast to INC dielectrics, where the thermal order-parameter fluctuations were observed only in a very narrow temperature range of a few tenths of a degree just below the phase transition.[24,25] The CDW phase fluctuations are performed on a scale small compared to the CDW wavelength, thus deeply in the subnanometric regime. Together with the low-fluctuation frequencies in the kHz range this clarifies why thermal fluctuations in the CDW systems were not directly observed so far.

V. CONCLUSIONS

The dynamics of an incommensurate CDW was studied in the absence of an external electric field. The decay of the

transverse nuclear-spin magnetization in a spatially inhomogeneous sinusoidal EFG has demonstrated that the CDW performs thermally induced incoherent phase fluctuations that result in a characteristic exponential NMR spin-echo decay with the exponent proportional to the time variable as $t^{3/2}$. Phase fluctuations of a pinned CDW are performed on a scale of a small fraction of the CDW wavelength, that is, on the subnanometric scale. The fluctuation frequencies are slow and affect the homogeneous NMR line shape that is sensitive to incoherent motions in the kHz range. The fluctuations are weakly temperature dependent and were observed in the blue bronze compound in the whole measured temperature range ($\approx$110 K) below the Peierls transition. These small-scale slow phase fluctuations very likely result from the partial thermal depinning-repinning process of the CDW at impurity- or commensurability-induced pinning centers, resembling a diffusive random walk. Such small-scale slow motions are extremely difficult to observe, and we believe that the present study presents—to the best of our knowledge—the first direct experimental observation of thermal fluctuations in the CDW systems. The existence of thermal fluctuations supports the hypothesis that at finite temperatures the CDW can reach an overall ground state even in the presence of randomly distributed impurities and weak external electric field and is not trapped into a spin-glass–like metastable state forever, as expected at zero temperature. Thermal fluctuations essentially present a mechanism for selecting between different metastable states that is absent at $T=0$ and drives the combined CDW-impurity system towards a global ground state. The above described NMR method for the detection of thermal fluctuations should be directly applicable also to other systems in which the thermal motion of superstructures is of interest. Among these are spin-density-wave systems, modulated magnetic structures, and vortex lattices in type-II superconductors.

ACKNOWLEDGMENTS

Blue-bronze crystals were synthesized in the laboratory of Professor T. Sambongi at Hokkaido University during the realization of the research program of K.B. supported by Matsumae International Foundation.

[1] H. Fröhlich, Proc. R. Soc. London, Ser. A **223**, 296 (1954).
[2] For a review, see P. Monceau, in *Electronic Properties of Inorganic Quasi-One-Dimensional Compounds, Part II*, edited by P. Monceau (Reidel, Dordrecht, 1985), pp. 139–268.
[3] A. Janossy, C. Berthier, and P. Segrans, Phys. Scr. **T19**, 578 (1987).
[4] J. Dumas, A. Arbaoui, H. Guyot, J. Marcus, and C. Schlenker, Phys. Rev. B **30**, 2249 (1984).
[5] A. Janossy, C. Berthier, P. Segrans, and P. Butaud, Phys. Rev. Lett. **59**, 2348 (1987).
[6] P. Bak and S. A. Brazovsky, Phys. Rev. B **17**, 3154 (1978).
[7] H. Fukuyama and P. A. Lee, Phys. Rev. B **17**, 535 (1978).
[8] P. A. Lee and T. M. Rice, Phys. Rev. B **19**, 3970 (1979).
[9] H. Fukuyama, J. Phys. Soc. Jpn. **41**, 513 (1976).
[10] Y. Okabe and H. Fukuyama, Solid State Commun. **20**, 345 (1976).
[11] N. Teranishi and R. Kubo, J. Phys. Soc. Jpn. **47**, 720 (1979).
[12] J. P. Pouget, B. Hennion, C. Escribe-Filippini, and M. Sato, Phys. Rev. B **43**, 8421 (1991).
[13] D. S. Fisher, Phys. Rev. B **31**, 1396 (1985).
[14] P. Lederer, G. Montambaux, J. P. Jamet, and M. Chauvin, J. Phys. (Paris) Lett. **45**, L627 (1984).
[15] J. R. Tucker, Phys. Rev. Lett. **60**, 1574 (1988).
[16] J. H. Ross, Jr., Z. Wang, and C. P. Slichter, Phys. Rev. Lett. **56**, 663 (1986).
[17] V. A. Golovko, and A. P. Levanyuk, in *Light Scattering Near Phase Transitions*, edited by H. Z. Cummins and A. P. Levanyuk, Modern Problems in Condensed Matter Science Vol. 5 (North-Holland, Amsterdam, 1983), pp. 169–225.
[18] V. A. Golovko and A. P. Levanyuk, in *Light Scattering Near Phase Transitions* (Ref. 17), p. 196.
[19] V. A. Golovko and A. P. Levanyuk, in *Light Scattering Near Phase Transitions* (Ref. 17), p. 193.
[20] R. Blinc, Phys. Rep. **79**, 333 (1981).
[21] A. Abragam, *Principles of Nuclear Magnetism* (Oxford University, Oxford, 1986), p. 432.
[22] J. Dolinšek, J. Magn. Reson. **92**, 312 (1991).
[23] J. P. Pouget, C. Noguera, A. H. Moudden, and R. Moret, J. Phys. (Paris) **46**, 1731 (1985).
[24] A. M. Fajdiga, T. Apih, J. Dolinšek, R. Blinc, A. P. Levanyuk, S. A. Minyukov, and D. C. Ailion, Phys. Rev. Lett. **69**, 2721 (1992).
[25] J. Dolinšek, A. M. Fajdiga-Bulat, T. Apih, R. Blinc, and D. C. Ailion, Phys. Rev. B **50**, 9729 (1994).